52nd IEEE Conference on Decision and Control
December 10-13, 2013. Florence, Italy

Regularization-Based Identification for Level Set Equations

Insoon Yang Claire J. Tomlin

Abstract— **An optimization-based method for identifying the speed profile of a moving surface from image data is studied. If the dynamic surface motion is modeled by a level set equation, the identification problem can be formulated as an optimization problem constrained with the level set equation whose (viscosity) solution, in general, has kinks. The non-differentiable solution prevents us from having a bounded gradient of the cost function of the optimization problem. To overcome this difficulty, we develop a novel identification approach using a regularized level set equation. The regularization guarantees the differentiability of the cost function and the boundedness of the gradient. Using numerical optimization techniques with the adjoint-based gradient, we solve the identification problem. We perform a numerical test to validate that the solution of an optimization problem with a regularized level set equation converges to the solution of the same optimization problem with an unregularized level set equation as the regularization factor tends to zero. The performance and usefulness of the method are demonstrated by a biological example in which we estimate the forces (per density) of actin and myosin in cell polarization.**

I. Introduction

The level set equation has been recognized as one of the most popular partial differential equation (PDE) models due to its many applications [1], [2], [3]. In particular, the level set equation provides a good modeling framework for the motion of a surface (or a curve). More precisely, the surface can be represented by the zero level set of the solution to the level set equation. Several level set equation-based models that describe surface motions are used in computer vision [4], computer graphics [5], multi-phase physics [6] and spatial systems biology [7]. One of the most important basic level set equation models is a Hamilton-Jacobi equation that describes the evolution of the surface in the normal direction of its boundary with the speed profile distributed over the boundary [2], [3]: it models, for example, the balance between the adhesion and the normal protrusion (or contraction) forces in a biological cell boundary [7], [8].

Given image data or video of a surface motion, it is often important to identify the speed profile of the surface. For example, the speed profile of cell surfaces has drawn great interests in the study of cancer, as the role of cell morphological changes in malignant transformations is investigated [9]. The identification of the speed profile when the cell surface is changing in its normal direction (e.g., the motion under the balance between the adhesion and normal protrusion forces) is a preliminary step for identifying it in more complicated cell morphology changes in carcinogenesis or metastasis. If we describe the dynamics of the surface with a level set equation, then the speed profile of the surface motion can be identified by solving a PDE-constrained optimization problem. The cost function of the optimization problem represents the difference between the solution of the level set equation and the given data, and the constraint of the problem is the level set equation.

In general, PDE-constrained optimization problems can be efficiently solved with nonlinear programming algorithms if an analytic form of the gradient of the cost function is provided [10]. A popular approach for deriving an analytic formula for the gradient is an *adjoint-based method*, and this method is also a classical method for the parameter optimization of ordinary differential equation (ODE) models [11]. The adjoint-based method for PDE-constrained optimization problems requires more careful analysis than ODE-constrained optimization problems because the solution of the PDEs does not always have enough differentiability and regularity to guarantee the existence of a well-defined gradient. Furthermore, the differentiability and regularity of the solution highly depend on the type of the PDE: therefore, the method has been customized to several types of PDEs and used in relevant applications [12], [13], [14], [15], [16], [17].

In this paper, we study the identification problem of the speed profile such that the level set equation best matches the desired data. The most relevant work is [18], in which *particle markers* on the surface are employed to estimate the speed profile. However, the particle marker-based method is not able to compute the speed in the normal direction when marker paths cross. An optical flow velocity based on image gradients is used in [19] when topological changes of the surface do not occur. The method proposed in this paper is a fully Eulerian method that does not use particle markers and is robust to topological changes of the surface; it solves a PDE-constrained optimization problem to identify the speed profile. To the best of our knowledge, an optimization-based identification method for the level set equation that describes the surface motion in its normal direction has not been explored. The cost function of the optimization problem is not differentiable with respect to the speed function because the (viscosity) solution is not differentiable everywhere: the non-differentiability of the cost function prevents us from employing a gradient-based algorithm. To overcome this limitation, we develop a novel identification approach

This work was supported by the NCI PS-OC program under grant number 29949-31150-44-IQPRJ1-IQCLT and by the NSF CPS project ActionWebs under grant number 0931843.

I. Yang and C. J. Tomlin are with the Department of Electrical Engineering and Computer Sciences, University of California, Berkeley, CA 94720, USA {iyang, tomlin}@eecs.berkeley.edu

C. J. Tomlin is also with the Life Sciences Division, Lawrence Berkeley National Laboratory, Berkeley, CA 94720, USA

utilizing a regularized level set equation. Our method has two important features. First, we use a regularized level set equation whose solution converges to the viscosity solution of the original level set equation; this approach permits us to employ the boundedness of the regularized solution and its first derivatives. Both the differentiability and the regularity of the regularized solution play a critical role in ensuring the differentiability of the cost function. Second, we propose an adjoint equation of the regularized level set equation that is associated with the optimization problem under consideration. The regularization also allows the adjoint equation to have a square-integrable weak solution. We derive an analytic formula for the gradient of the cost function utilizing the adjoint equation and show that the gradient is bounded. Furthermore, we perform a numerical test to validate that the solution of an optimization problem that uses a regularized level set equation converges to the solution of the original optimization problem as the regularization factor tends to zero. An example that identifies the forces (per density) of actin and myosin in cell morphology change demonstrates the performance of the proposed method and the potential usefulness of the method in the estimation of cellular mechanical properties from image data or movies.

II. Level Set Equation for a Dynamic Surface Moving in Its Normal Direction

Consider a surface $\Gamma(t)$ that moves over time for $t \in [0,T]$ in a bounded and open domain $\Omega \subset \mathbb{R}^3$. Suppose that the surface separates one region from another, and evolves in the direction that is normal to its boundary with the speed $F : \Omega \to \mathbb{R}$. If the surface moves in the outward normal direction at $\boldsymbol{x} := (x,y,z) \in \Omega$, then $F(\boldsymbol{x})$ is positive; however, if it moves in the inward normal direction at $\boldsymbol{x}$, then $F(\boldsymbol{x})$ is negative. Let $\Omega^-(t)$ and $\Omega^+(t)$ be open subsets of the domain Ω that represent the volumes inside and outside of the surface $\Gamma(t)$, respectively. Note that Ω is a disjoint union of $\Omega^-(t)$, $\Gamma(t)$ and $\Omega^+(t)$ for all $t \in [0,T]$. An example that depicts $\Gamma(t)$, $\Omega^-(t)$ and $\Omega^+(t)$ is shown in Fig. 1. We choose a level set function $\phi_0 : \Omega \to \mathbb{R}$ as

$$\phi_0(\boldsymbol{x}) \begin{cases} < 0 & \text{if } \boldsymbol{x} \in \Omega^-(0) \\ = 0 & \text{if } \boldsymbol{x} \in \Gamma(0) \\ > 0 & \text{if } \boldsymbol{x} \in \Omega^+(0). \end{cases}$$

For the sake of simplicity, suppose that ϕ_0 is a smooth function.

We now consider the following Hamilton-Jacobi PDE with $\phi : \Omega \times [0,T] \to \mathbb{R}$:

$$\phi_t + H(\nabla\phi, F) = 0 \quad \text{in } \Omega \times [0,T], \tag{1a}$$
$$\phi(\boldsymbol{x},0) = \phi_0(\boldsymbol{x}) \quad \text{in } \Omega \times \{t=0\}, \tag{1b}$$

with the Hamiltonian

$$H(\nabla\phi, F) = F\|\nabla\phi\|. \tag{2}$$

We call (1) the *level set equation* [1], and we assume periodic boundary conditions. An important feature of the level set equation is that the zero-level set of $\phi(\cdot,t)$ corresponds to the surface $\Gamma(t)$ that moves in the normal direction with the speed function F for all time t. More precisely, the level set function has the following property:

$$\boldsymbol{x} \in \begin{cases} \Gamma(t) & \text{if } \phi(\boldsymbol{x},t) = 0 \\ \Omega^-(t) & \text{if } \phi(\boldsymbol{x},t) < 0 \\ \Omega^+(t) & \text{if } \phi(\boldsymbol{x},t) > 0. \end{cases}$$

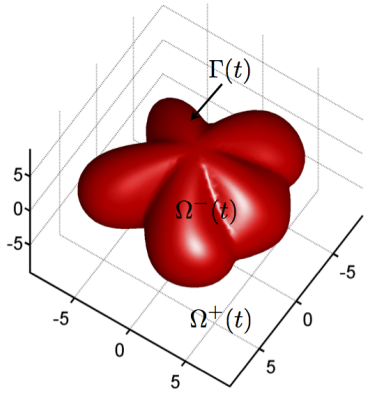

Fig. 1: The subdomain $\Omega^-(t)$ is the region enclosed by the surface $\Gamma(t)$; and $\Omega^+(t) = \Omega \setminus (\Omega^-(t) \cup \Gamma(t))$.

The level set equation implicitly tracks the motion of the surface Γ by computing the evolution of the level set function ϕ rather than explicitly track the motion of Γ, as in the Lagrangian framework. Computational modeling of the dynamic surface motion with the level set equation has practical advantages: first, the level set method for solving (1) does not result oscillation of the surface unlike Lagrangian methods (e.g. particle marker); second, the level set method naturally handles topological changes of the surface [2], [3].

The fact that the solution of (1) is not generally differentiable everywhere motivates weak solutions of (1). Among these weak solutions, the *viscosity solution* is sophisticatedly designed so that it has the properties of uniqueness and consistency. For a detailed definition and investigation of viscosity solutions, we refer the reader to [20], [21]. We seek to identify the speed function F of the surface in the Hamiltonian such that the level set equation models the given data of the surface motion well. Our approach minimizes a cost function that measures the difference between Γ and the given data by using the gradient of this cost function with respect to F. Although we can fully benefit from the properties of uniqueness and consistency when we use the viscosity solution, its non-differentiability could be problematic in defining and computing the gradient of the cost function. To overcome this limitation, we utilize a regularized level set equation.

A. Regularization

Consider the regularized level set equation of the form [22]

$$\phi^\epsilon_t + H(\nabla\phi^\epsilon, F) = \epsilon\Delta\phi^\epsilon \quad \text{in } \Omega \times [0,T], \tag{3a}$$
$$\phi^\epsilon(\boldsymbol{x},0) = \phi_0(\boldsymbol{x}) \quad \text{in } \Omega \times \{t=0\}, \tag{3b}$$

with the same Hamiltonian as (2), where $\epsilon > 0$ is the regularization factor. For the sake of simplicity, we assume that $\epsilon \in (0,1)$. Then, there exists a unique bounded solution ϕ^ϵ such that its first derivatives are bounded for any $T > 0$, i.e.,

$$\sup_{\Omega\times[0,T]} |\phi^\epsilon|, \|\nabla\phi^\epsilon\|, |\phi_t^\epsilon| \le C \tag{4}$$

for some constant C [22]. In addition, this regularized solution also converges to the viscosity solution ϕ of (1) locally uniformly [20], i.e.,

$$\phi^\epsilon \to \phi \quad \text{as } \epsilon \to 0. \tag{5}$$

This convergence result justifies the use of the regularized level set equation (3) with a very small $\epsilon > 0$ instead of (1) to identify F. Although ϕ^ϵ converges to ϕ locally uniformly, the regularization factor $\epsilon > 0$ could be a source of numerical errors in the identification of F. By performing numerical experiments in Section IV, we validate that the optimal F in the regularized equation (3) converges to the optimal F in the original equation (1) as ϵ approaches zero. This regularization has two major advantages: first, the cost function with the regularized solution is differentiable as we will show in Section III-C. Therefore, the gradient of this cost function exists and is unique. Second, the boundedness of the regularized solution and its derivatives guarantees the boundedness of the gradient of the cost function, as we will show in the next section. The bounded gradient plays a critical role in optimization algorithms because it prevents the termination of the algorithms before an optimum is found. Therefore, regularization eventually allows us to solve optimization problems without a potential failure caused by unbounded gradients.

III. Variational Method For Identification

Recall that the speed $F = F(\boldsymbol{x})$ that we want to identify is a function of space. We choose the space of feasible speed functions as $\mathcal{F} = L^\infty(\Omega)$ because in practice the function must be essentially bounded. Let $\Gamma^D(t)$, $t \in [0,T]$ be the position data of the surface and let $\Omega^{D-}(t)$ and $\Omega^{D+}(t)$ be the inner and outer volumes of the surface $\Gamma^D(t)$, respectively. Then, we can numerically construct a level set function $\phi^D(\,\cdot\,,t)$ whose zero level set and zero sublevel set coincide with $\Gamma^D(t)$ and $\Omega^{D-}(t)$, respectively [23], [24]. Our goal is to find the speed function $F \in \mathcal{F}$ such that the zero level set of the solution of (3) matches Γ^D as well as possible. To this end, we pose the following optimization problem:

$$\min_{F\in\mathcal{F}} \; J^\epsilon(F) = \frac{1}{2}\int_0^T \int_\Omega [S(\phi^\epsilon) - S(\phi^D)]^2 \, d\boldsymbol{x}dt \tag{6a}$$

$$\text{subject to } \textbf{regularized level set equation } (3) \tag{6b}$$

$$F_L \le F(\boldsymbol{x}) \le F_U, \quad \forall \boldsymbol{x} \in \Omega, \tag{6c}$$

where $S : \mathbb{R} \to [0,1]$ is a smooth approximation of the Heaviside step function. As in [17], we set

$$S(p) = \frac{1}{2} + \frac{1}{2}\tanh\left(\frac{p}{\tau}\right), \tag{7}$$

for a small $\tau > 0$. As we showed in [17], the cost function measures the volume of the non-overlapping regions between Ω^- and Ω^{D-}.

Lemma 1: As $\tau \to 0^+$, we have

$$\int_\Omega \left[S(\phi(\boldsymbol{x},t)) - S(\phi^D(\boldsymbol{x},t))\right]^2 \, d\boldsymbol{x} \to |\Omega^-(t) - \Omega^{D-}(t)| = |\Omega^+(t) - \Omega^{D+}(t)|.$$

We refer to [17] for the proof of the lemma. Lemma 1 implies that the optimal solution to (6) minimizes the difference between Ω^- and Ω^{D-} when $\tau \to 0^+$. Using $\tau > 0$ may introduce errors in the optimal solution because we minimize the approximated difference between Ω^- and Ω^{D-}. However, a sufficiently small $\tau > 0$ does not significantly deteriorate the accuracy of the optimal solution in our numerical tests. The primary reason why we use a positive τ is that it allows the differentiability of the cost function J^ϵ; in contrast, $\tau = 0$ renders the cost function non-differentiable. If the cost function is differentiable, then we can use its gradient to solve the optimization problem with efficient nonlinear programming algorithms that allow super-linear convergence by utilizing approximate Hessian matrix information. To demonstrate the differentiability of the cost function and to derive the formula for the gradient, we will use the variational approach that we propose below.

A. First variation

We begin by considering the variation $F + \tilde{F} \in \mathcal{F}$ of the speed function F such that

$$\|\tilde{F}\| := \int_\Omega |\tilde{F}(\boldsymbol{x})|^2 \, dx \le C,$$

for some constant C. We use the notation $\phi^\epsilon[F]$ to denote the solution of (3) with the speed function F. Let $\tilde{\phi}^\epsilon := \phi^\epsilon[F+\tilde{F}] - \phi^\epsilon[F]$. Then, it solves the following nonlinear PDE: in $\Omega \times [0,T]$,

$$\tilde{\phi}_t^\epsilon + F\frac{\nabla\phi^\epsilon}{\|\nabla\phi^\epsilon\|}\cdot\nabla\tilde{\phi}^\epsilon + \tilde{F}\|\nabla\phi^\epsilon\| + f^\epsilon = \epsilon\Delta\tilde{\phi}^\epsilon, \tag{8}$$

where f^ϵ absorbs the higher-order terms in the Taylor expansion of the Hamiltonian H, i.e.,

$$f^\epsilon := \int_0^1 (1-s)\left(\tilde{v}^\top D^2 H(v + s\tilde{v})\tilde{v}\right) \, ds$$

due to the mean value theorem, where $v := (\nabla\phi^\epsilon, F)$ and $\tilde{v} := (\nabla\tilde{\phi}^\epsilon, \tilde{F})$. The initial value is zero, i.e., $\tilde{\phi}^\epsilon(\,\cdot\,,0) = 0$. Intuitively, $\tilde{\phi}$ tends to zero as $\tilde{F}$ approaches zero in $\mathcal{F}$. In fact, we have obtained a stronger estimate, which is presented in the following proposition.

Proposition 1: Let $\tilde{\phi}^\epsilon := \phi^\epsilon[F+\tilde{F}] - \phi^\epsilon[F]$. Then,

$$\int_0^T\int_\Omega |\tilde{\phi}^\epsilon(\boldsymbol{x},t)|^2 \, d\boldsymbol{x}dt \le K\int_\Omega |\tilde{F}(\boldsymbol{x})|^2 \, d\boldsymbol{x} \tag{9}$$

for some constant K that is independent of $\tilde{F}$.

A detailed proof can be found in the long version [25]. The ϵ-regularization and Proposition 1 allow us to go beyond the estimate for $\tilde{\phi}^\epsilon$: we have the additional estimate for $\nabla\tilde{\phi}^\epsilon$, which is proposed in the next proposition.

Proposition 2: Let $\tilde{\phi}^\epsilon := \phi^\epsilon[F+\tilde{F}] - \phi^\epsilon[F]$. Then,

$$\int_0^T \int_\Omega \|\nabla\tilde{\phi}^\epsilon(\boldsymbol{x},t)\|^2 \, d\boldsymbol{x}dt \le K \int_\Omega |\tilde{F}(\boldsymbol{x})|^2 \, d\boldsymbol{x}, \qquad (10)$$

for some constant K that is independent of $\tilde{F}$.

For the proof of the proposition, please refer to the long version [25]. Propositions 1 and 2 play a critical role in proving the differentiability of J^ϵ and in deriving the formula for $\nabla_F J^\epsilon$. Roughly speaking, these propositions control the higher-order terms of $J^\epsilon(F+\tilde{F}) - J^\epsilon(F)$ in $\tilde{\phi}^\epsilon$ and $\nabla\tilde{\phi}^\epsilon$ in the derivation of $\nabla_F J^\epsilon$. Before we examine the gradient, we introduce an adjoint equation for the optimization problem (6).

B. Adjoint equation

We define the *adjoint equation* of the regularized level set equation (3) that is associated with the optimization problem (6) as

$$-\mu_t^\epsilon - \nabla\cdot\left(F\frac{\nabla\phi^\epsilon}{\|\nabla\phi^\epsilon\|}\mu^\epsilon\right) = \epsilon\Delta\mu^\epsilon + G \text{ in } \Omega\times[0,T], \qquad (11a)$$

$$\mu^\epsilon(\boldsymbol{x},T) = 0 \text{ in } \Omega\times\{t=0\}, \qquad (11b)$$

where $G := -(S(\phi^\epsilon) - S(\phi^D))S'(\phi^\epsilon)$ and the boundary condition is periodic. In addition, the adjoint state μ^ϵ can be interpreted as the dual variable of the solution to the regularized level set equation (3). The adjoint equation will be used in the derivation of the gradient $\nabla_F J^\epsilon$ in the following section.

We note that the condition (11b) is the terminal condition. Thus, we need to solve the equation backward in time. If we perform a change of variable as $\zeta(\cdot,t) = \mu(\cdot,T-t)$, then we can interpret the equation as an *reaction-advection-diffusion equation* with the velocity field $-F\nabla\phi^\epsilon/\|\nabla\phi^\epsilon\|$, the diffusion coefficient ϵ, and the reaction function G. It is well known that the reaction-advection-diffusion type equation has a unique weak solution such that

$$\int_0^T \int_\Omega |\mu^\epsilon|^2 \, d\boldsymbol{x}dt \le C \qquad (12)$$

for some constant C [26].

C. Gradient

We are ready to show the differentiability of the cost function J^ϵ and to derive an expression for $\nabla_F J^\epsilon$ using the estimate result in Section III-A and the adjoint equation in Section III-B. Note that we study the differentiability of a functional (J^ϵ) with respect to a function (F) in a Banach space ($\mathcal{F} = L^\infty(\Omega)$). The Fréchet differentiability provides a bound of the variation of the functional with respect to an arbitrary variation of the function, while the Gâteaux differentiability does so only if the function varies in a certain direction. Therefore, we examine the Fréchet differentiability to allow an arbitrary variation of F in a numerical algorithm to solve (6).

Theorem 1: The cost function J^ϵ is Fréchet differentiable. Furthermore, the gradient of J^ϵ with respect to the speed function F is given by

$$\nabla_F J^\epsilon = \int_0^T \int_\Omega \|\nabla\phi^\epsilon\|\mu^\epsilon \, d\boldsymbol{x}dt, \qquad (13)$$

where ϕ^ϵ and μ^ϵ are solutions of (3) and (11), respectively. Furthermore, the gradient is bounded.

Proof: We introduce the notation $\boldsymbol{O} := O(\|\tilde{F}\|^2) + O(\|\tilde{\phi}^\epsilon\|^2_{L^2(\Omega\times(0,T))}) + O(\|\nabla\tilde{\phi}^\epsilon\|^2_{L^2(\Omega\times(0,T))})$ to represent any higher-order terms in $\tilde{F}, \tilde{\phi}^\epsilon$, and $\nabla\tilde{\phi}^\epsilon$. Propositions 1 and 2 suggest that $\boldsymbol{O}/\|\tilde{F}\| \to 0$ as $\tilde{F}\to 0$ in $\mathcal{F}$. First, we consider the difference

$$\begin{aligned} &J^\epsilon(F+\tilde{F}) - J^\epsilon(F) \\ &\quad = \int_0^T\int_\Omega (S(\phi^\epsilon) - S(\phi^D))S'(\phi^\epsilon)\tilde{\phi}^\epsilon \, d\boldsymbol{x}dt + \boldsymbol{O}, \end{aligned} \qquad (14)$$

as $\tilde{F}\to 0$ in $\mathcal{F}$, which is the result of a Taylor expansion. Note that this Taylor expansion is valid because the approximate Heaviside step function S is differentiable. Multiply the left-hand side of (8) by the adjoint state μ, integrate this product over $\Omega\times(0,T)$, and add this integral, which is zero, to the difference (14). Then, as $\tilde{F}\to 0$ in $\mathcal{F}$, we have

$$\begin{aligned} &J^\epsilon(F+\tilde{F}) - J^\epsilon(F) \\ &= \int_0^T\int_\Omega (S(\phi^\epsilon) - S(\phi^D))S'(\phi^\epsilon)\tilde{\phi}^\epsilon \, d\boldsymbol{x}dt + \boldsymbol{O} \\ &+ \int_0^T\int_\Omega \mu^\epsilon\left(\tilde{\phi}_t^\epsilon + F\frac{\nabla\phi^\epsilon}{\|\nabla\phi^\epsilon\|}\cdot\nabla\tilde{\phi}^\epsilon + \tilde{F}\|\nabla\phi^\epsilon\| - \epsilon\Delta\tilde{\phi}^\epsilon\right) d\boldsymbol{x}dt. \end{aligned}$$

Using integration by parts and the divergence theorem with periodic boundary conditions, we obtain

$$\int_0^T \mu^\epsilon\tilde{\phi}_t^\epsilon dt = -\int_0^T \mu_t^\epsilon\tilde{\phi}dt, \quad \int_\Omega \mu^\epsilon\Delta\tilde{\phi}^\epsilon d\boldsymbol{x} = \int_\Omega \Delta\mu^\epsilon\tilde{\phi}^\epsilon d\boldsymbol{x},$$

$$\int_\Omega \mu^\epsilon F\frac{\nabla\phi^\epsilon}{\|\nabla\phi^\epsilon\|}\cdot\nabla\tilde{\phi}^\epsilon \, d\boldsymbol{x} = -\int_\Omega \nabla\cdot\left(\mu^\epsilon F\frac{\nabla\phi^\epsilon}{\|\nabla\phi^\epsilon\|}\right)\tilde{\phi}^\epsilon \, d\boldsymbol{x}.$$

By substituting these equations into the previous formula for the difference, we obtain

$$\begin{aligned} J^\epsilon(F+\tilde{F}) - J^\epsilon(F) &= \int_0^T\int_\Omega \mu^\epsilon\|\nabla\phi^\epsilon\|\tilde{F}\, d\boldsymbol{x}dt + \boldsymbol{O} \\ &+ \int_0^T\int_\Omega \left[-\mu_t^\epsilon - \nabla\cdot\left(\mu^\epsilon F\frac{\nabla\phi^\epsilon}{\|\nabla\phi^\epsilon\|}\right) - \epsilon\Delta\mu^\epsilon \right. \\ &\qquad \left. + (S(\phi^\epsilon) - S(\phi^D))S'(\phi^\epsilon)\right]\tilde{\phi}^\epsilon \, d\boldsymbol{x}dt. \end{aligned}$$

Note that, due to the adjoint equation (11), the second integral in the above equation is zero. Let $D_F J^\epsilon(F:\tilde{F}) := \int_0^T\int_\Omega \mu^\epsilon\|\nabla\phi^\epsilon\|\tilde{F}\, d\boldsymbol{x}dt$. Recall that $\boldsymbol{O}/\|\tilde{F}\| \to 0$ as $\tilde{F}\to 0$. Consequently, we obtain

$$\frac{\|J^\epsilon(F+\tilde{F}) - J^\epsilon(F) - D_F J^\epsilon(F:\tilde{F})\|}{\|\tilde{F}\|} \to 0,$$

as $\tilde{F}\to 0$ in $\mathcal{F}$, which implies that J^ϵ is Fréchet differentiable and that $D_F J^\epsilon(F:\tilde{F})$ is indeed the Fréchet derivative of J^ϵ with respect to F. Therefore, we conclude that the gradient can be obtained as (13). Recall the estimates (4) and (12) of the primal and the adjoint states, respectively. Using these estimates, we have the boundedness of the gradient. ■

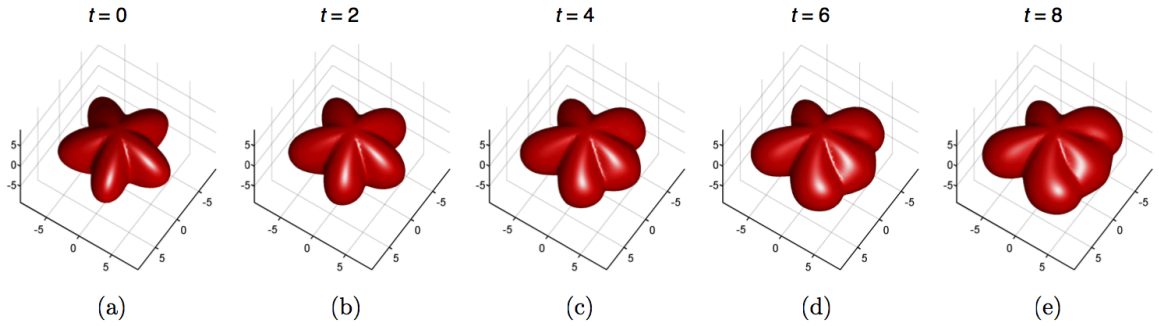

Fig. 2: The data for the surface evolution $\Gamma(t)$, $t = 0, 2, 4, 6, 8$.

Note that Propositions 1 and 2 control all of the higher-order terms in $\tilde{\phi}^\epsilon$ and $\nabla\phi^\epsilon$, and therefore, $\boldsymbol{O}/\|\tilde{F}\|$ approaches zero as $\tilde{F}$ tends to zero in $\mathcal{F}$. This fact guarantees the differentiability of the cost function. Furthermore, in the difference $J^\epsilon(F+\tilde{F}) - J^\epsilon(F)$, the adjoint equation transfers the effect of $\tilde{\phi}^\epsilon$ to the adjoint state μ^ϵ.

D. Algorithm

When we numerically optimize F, we should discretize $F \in \mathcal{F}$ over space and optimize its value on the resulting nodes, distributed over Ω. It is convenient to introduce the basis functions $\{\beta_m(\cdot)\}_{m=1}^M \in L^\infty(\Omega)$ for $F(\cdot)$, i.e., for $\boldsymbol{x} \in \Omega$,

$$F(\boldsymbol{x}) := \sum_{m=1}^{M} w_m \beta_m(\boldsymbol{x}),$$

where $w_m \in \mathbb{R}$ is the basis weight for $\beta_m : \Omega \to \mathbb{R}_+$. Let $w := (w_1, \cdots, w_M)^\top$ and let $\beta := (\beta_1, \cdots, \beta_M)^\top$. If we want to evaluate F at all of the nodes as in finite element methods or finite difference methods, for example, we can use the piecewise linear basis functions $\{\beta_m(\cdot)\}_{m=1}^M$ such that

$$\beta_m(\boldsymbol{x}_i) = \begin{cases} 1 & \text{if } i = m, \\ 0 & \text{otherwise.} \end{cases}$$

These basis functions are defined at each node, i.e., M is the number of nodes. Given the basis functions β, we identify the basis weights such that the level set equation best describes the evolution of a surface, which is given in the form of data. Due to Theorem 1, we can derive the gradient of the cost function with respect to the basis weight as

$$\nabla_w J^\epsilon = \int_0^T \int_\Omega \beta \|\nabla\phi^\epsilon\| \mu^\epsilon \, d\boldsymbol{x}dt. \tag{15}$$

The differentiability of the cost function and the analytic formula for its gradient allow us to use gradient-based nonlinear programming methods. In general, methods that use the gradient information are more efficient than those methods that do not use the gradient information [27]. Because the gradient formula (13) depends on both the primal and the adjoint states, we need to evaluate both states by numerically solving (3) and (11) to compute the gradient. The pseudo-algorithm to solve the optimization problem (6) using the gradient information is as follows:

1) Initialize w.
2) Numerically solve the regularized level set equation (3) to obtain the primal state ϕ^ϵ.
3) Numerically solve the adjoint equation (11) to obtain the adjoint state μ^ϵ.
4) Evaluate the gradient $\nabla_w J^\epsilon$ at w using (15).
5) Evaluate the gradients of the inequality constraints (6c).
6) Compute the descent direction and the step size using the gradients obtained in Steps 4 and 5 with an appropriate nonlinear programming method.
7) Update w using the descent direction and step size. Return to Step 2 if the convergence criteria do not hold.

In Step 2, we use numerical methods called the level set methods [1], [2], [3] to solve the (regularized) level set equation. These methods accurately approximate the surface motion with an entropy-satisfying numerical scheme for Hamilton-Jacobi PDEs, and they also conveniently use a Cartesian grid. For the adjoint equation, we use the upwind approximation of the advection term and the centered difference for the diffusion term [28]. Note that we must solve the adjoint equation backward in time. To determine the descent direction and the step size in Step 6, we can employ a number of nonlinear programming methods such as interior-point methods, sequential quadratic programming (SQP) methods, conjugate-gradient methods, and trust-region methods. In our numerical tests, an interior-point algorithm that hybridizes the line search and conjugate gradient trust-region methods is used [29], [30].

IV. Numerical Tests

A. Convergence test

We have shown that the ϵ-regularization in (3) plays a critical role in proving the differentiability of the cost function. The gradient ∇J^ϵ is the key ingredient of the algorithm that solves the optimization problem (6). Let $w^{*\epsilon}$ denote the numerical solution of the problem that is obtained using the algorithm in the previous section with the gradient ∇J^ϵ. Although ϕ^ϵ converges to ϕ as ϵ tends to zero, it is unclear whether $w^{*\epsilon}$ converges to w^*, which is the solution of the optimization problem (6) with $\epsilon = 0$. In this section, we perform the test for the numerical convergence of $w^{*\epsilon}$

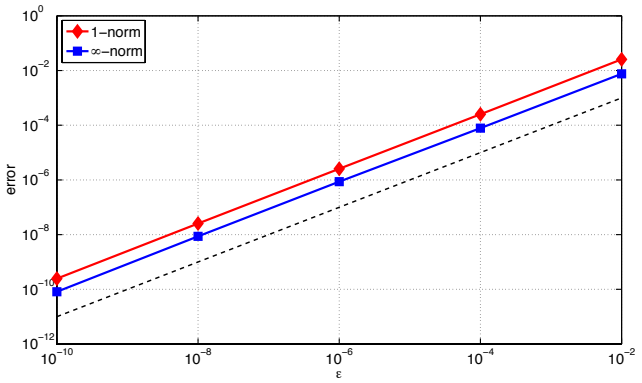

Fig. 3: The errors in the 1- and ∞-norms with respect to the regularization factor ϵ. The dotted line is the reference line with a slope of 1 in the log-log scale.

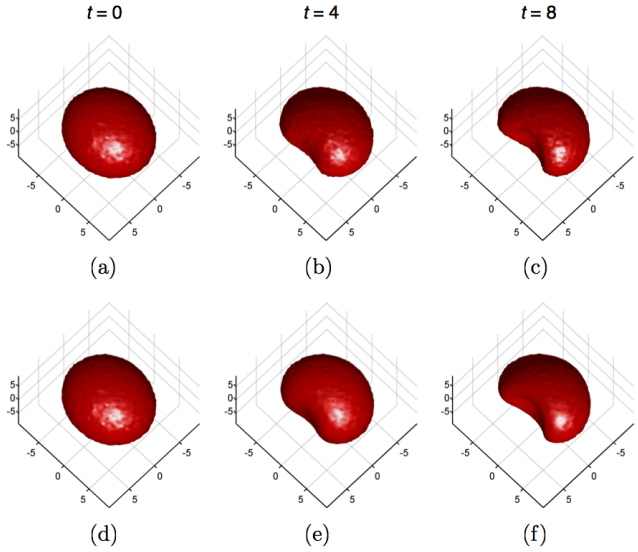

Fig. 4: (a)–(c) The data from the cell morphology change $\Gamma^D(t)$, $t = 0, 4, 8$. (d)–(f) The cell morphology change $\Gamma(t)$, $t = 0, 4, 8$ that is predicted by the level set equation with identified parameters.

to w^*. To that end, we first set the ground truth weight $w^* = (-0.0782, 0.4157, 0.2922, 0.4595)$ for the radial basis functions $\beta_k(\boldsymbol{x}) = \exp(-\|\boldsymbol{x} - \boldsymbol{x}_k\|^2/10)$, where $\boldsymbol{x}_1 = (-5, -5, 0)$, $\boldsymbol{x}_2 = (-5, 5, 0)$, $\boldsymbol{x}_3 = (5, -5, 0)$, and $\boldsymbol{x}_4 = (5, 5, 0)$. By numerically solving the level set equation (1) with the function F that is constructed by the basis functions and the ground truth weights, we obtain the synthetic data ϕ^D and Γ^D for $t \in [0, 8]$. In Fig. 2, $\Gamma^D(t)$, $t = 0, 2, 4, 6, 8$ are displayed. In the numerical simulation, we choose the grid spacing as $h = 0.4$ and the time step as $\Delta t = 0.08$.

To study the effect of ϵ, we vary ϵ from 10^{-2} to 10^{-10} and compute the solution $w^{*\epsilon}$ of the optimization problem (6) where $(w_L, w_U) = (-0.5, 0.5)$. The smoothing factor τ in the smooth Heaviside step function (7) is selected as $0.01h$. Let e denote the numerical error of the solution, i.e.,

$$e^\epsilon := \|w^{*\epsilon} - w^*\|, \tag{16}$$

where w^* is the ground truth weight. We compute the errors in the 1- and ∞-norms. As shown in Fig. 3, the error converges to zero in both norms with the convergence rate 1. This convergence result suggests that the solution obtained by the regularization-based approach is a good approximation of the solution to the unregularized problem: furthermore, the sequence $\{w^{*\epsilon}\}$ is a converging sequence to w^*. This convergence property will be analytically studied in the future work.

B. Example: cell polarization via an actin-myosion system

The actin-myosin system is one of the critical factors that govern the dynamics of cell morphology. Actin cytoskeletons and actomyosin networks exert protrusive and contractile forces on the cell membrane, and these forces depend upon the cell's expansive and contractile movements, respectively. Despite a number of experiments, the relationship between the density of actin, V and the protrusive force, F_p is still arguable, as is the relationship between the density of myosin, W and the contractile force F_c. Several models for mapping from the density of actin and myosin (or the concentration of the proteins that are related to them) to these protrusive and retraction forces have been suggested [31], [8]. We use a simplified model [8] in which the forces are exerted in the direction that is normal to the cell boundary, i.e.,

$$F_p = aV\nu = aV\frac{\nabla\phi}{\|\nabla\phi\|}, \quad F_c = -bW\nu = -bW\frac{\nabla\phi}{\|\nabla\phi\|},$$

where a and b denote the magnitude of the force per density of actin and myosin, respectively. If we normalize the friction coefficient between the cell and its substrate to 1, then the following level set equation describes the dynamics of the cell boundary [7]:

$$\phi_t + (aV - bW)\|\nabla\phi\| = 0.$$

Note that we can naturally set the basis weights and basis functions as $w = (a, -b)$ and $\beta = (V, W)$, respectively.

Our goal is to identify a and b such that the level set model accurately describes the experimental data. In this example, we use synthetic data of cell morphology as shown in Figure 4 (a)–(c). To synthesize these data, we chose $w = (0.1, -0.8)$ and $\beta_k(\boldsymbol{x}) = \exp(-\|\boldsymbol{x} - \boldsymbol{x}_k\|^2/10)$, where $\boldsymbol{x}_1 = (-3.5, 0, 0)$ and $\boldsymbol{x}_2 = (3.5, 0, 0)$. We corrupt the solution values with the i.i.d. Gaussian noise $\mathcal{N}(0, 0.05)$. These synthetic data mimic the experimental data from the polarization of a cell due to an actin-myosin system [32]. To identify the parameters a and b, we solve the optimization problem (6) with $\epsilon = 10^{-6}$. We have tested several initial guesses of the parameters. The optimal solution that is obtained by the algorithm is quite robust with respect to the initial guesses (the errors $\|w^{*\epsilon} - w^*\|_1$ are all on the order of 10^{-3}). The comparison between the data and the dynamic surface with the identified speed profile is shown in Fig. 4.

V. Conclusion And Future Work

We have presented a novel regularization-based approach for identifying the speed function in a level set equation. The ϵ-diffusion term in the regularized level set equation played an essential role in ensuring both the differentiability of the cost function of the optimization problem and the boundedness of the gradient. The adjoint-based gradient allows us to efficiently solve the identification problem with a nonlinear programming algorithm. The numerical solution of the regularized problem converges to the solution of the unregularized problem as the regularization factor ϵ tends to zero. The regularization-based method successfully estimated the forces per density of actin and myosin that induces the dynamic change of a cell shape. We believe that the method will be very useful to estimate the mechanical properties of cells when direct experimental measurements of them are not tractable.

We plan to generalize our regularization-based method to any convex and non-convex Hamilton-Jacobi equations. This generalization will be useful in the sensitivity analysis of the value functions of optimal control and differential game problems.

References

[1] S. Osher and J. A. Sethian, "Fronts propagating with curvature-dependent speed: algorithms based on Hamilton-Jacobi formulations," *Journal of Computational Physics*, vol. 79, pp. 12–49, 1988.

[2] J. A. Sethian, *Level Set Methods and Fast Marching Methods: Evolving Interfaces in Computational Geometry, Fluid Mechanics, Computer Vision, and Materials Science*, 2nd ed. Cambridge University Press, New York, 1999.

[3] S. J. Osher and R. P. Fedkiw, *Level Set Methods and Dynamic Implicit Surfaces*, 1st ed. New York, NY: Springer, 2002.

[4] M. Niethammer, A. Tannenbaum, and S. Angenent, "Dynamic active contours for visual tracking," *IEEE Transactions on Automatic Control*, vol. 51, no. 4, pp. 562–579, 2006.

[5] J.-M. Hong, T. Shinar, and R. Fedkiw, "Wrinkled flames and cellular patterns," *ACM Transactions on Graphics*, vol. 26, no. 3, pp. 47–1 – 47–6, 2007.

[6] R. I. Saye and J. A. Sethian, "The Voronoi Implicit Interface Method for computing multiphase physics," *Proceedings of the National Academy of Sciences*, vol. 108, no. 49, pp. 19 498–19 503, 2011.

[7] L. Yang, J. C. Effler, B. L. Kutscher, S. E. Sullivan, D. N. Robinson, and P. A. Iglesias, "Modeling cellular deformations using the level set formalism," *BMC Systems Biology*, vol. 2, no. 68, pp. 1–16, 2008.

[8] D. Shao, W.-J. Rappel, and H. Levine, "Computational model for cell morphodynamics," *Physical Review Letters*, vol. 105, pp. 108 104–1 – 108 104–4, 2010.

[9] V. M. Weaver, O. W. Petersen, F. Wang, C. A. Larabell, P. Briand, C. Damsky, and M. J. Bissell, "Reversion of the malignant phenotype of human breast cells in three-dimensional culture and *in vivo* by integrin blocking antibodies," *The Journal of Cell Biology*, vol. 137, no. 1, pp. 231–245, 1997.

[10] M. Hinze, R. Pinnau, M. Ulbrich, and S. Ulbrich, *Optimization with PDE Constraints*. New York, NY: Springer, 2009.

[11] P. Kokotović and J. Heller, "Direct and adjoint sensitivity equations for parameter optimization," *IEEE Transactions on Automatic Control*, vol. 12, no. 5, pp. 609–610, 1967.

[12] H. T. Banks and K. Kunish, *Estimation Techniques for Distributed Parameter Systems*, 1st ed. Boston: Birkhäuser, 1989.

[13] C. Kravaris and J. H. Seinfeld, "Identification of parameters in distributed parameter systems by regularization," *SIAM Journal on Control and Optimization*, vol. 46, pp. 116–142, 1985.

[14] A. Jameson, "Aerodynamic design via control theory," *Journal of Scientific Computing*, vol. 3, no. 3, pp. 233–260, 1988.

[15] A. M. Bayen, R. L. Raffard, and C. J. Tomlin, "Adjoint-based control of a new Eulerian network model of air traffic flow," *IEEE Transactions on Control Systems Technology*, vol. 14, no. 5, pp. 804–818, 2006.

[16] D. Jacquet, M. Krstic, and C. C. de Wit, "Optimal control of scalar one-dimensional conservation laws," in *Proceedings of the 2006 American Control Conference*, Minneapolis, MN, USA, 2006.

[17] I. Yang and C. J. Tomlin, "Identification of surface tension in mean curvature flow," in *Proceedings of the 2013 American Control Conference*, Washington, DC, USA, 2013.

[18] M. Machacek and G. Danuser, "Morphodynamic profiling of protrusion phenotypes," *Biophysical Journal*, vol. 90, pp. 1439–1452, 2006.

[19] B. J. Dubin-Thaler, J. M. Hofman, Y. Cai, H. Xenias, I. Spielman, A. V. Shneidman, L. A. David, H.-G. Döbereiner, C. H. Wiggins, and M. P. Sheetz, "Quantification of cell edge velocities and traction forces reveals distinct motility modules during cell spreading," *PLoS One*, vol. 3, no. 11, pp. 1–15, 2008.

[20] M. G. Crandall and P.-L. Lions, "Viscosity solutions of Hamilton-Jacobi equations," *Transactions of the American Mathematical Society*, vol. 277, no. 1, pp. 1–42, 1983.

[21] M. G. Crandall, L. C. Evans, and P. L. Lions, "Some properties of viscosity solutoins of Hamilton-Jacobi equations," *Transactions of the American Mathematical Society*, vol. 282, no. 2, pp. 487–502, 1984.

[22] L. C. Evans, "On solving certain nonlinear partial differential equations by accretive operator methods," *Israel Journal of Mathematics*, vol. 36, pp. 225–247, 1980.

[23] J. A. Sethian, "A fast marching level set method for monotonically advancing fronts," *Proceedings of the National Academy of Sciences*, vol. 93, pp. 1591–1595, 1996.

[24] Y.-H. R. Tsai, "Rapid and accurate computation of the distance function using grids," *Journal of Computational Physics*, vol. 178, pp. 175–195, 2002.

[25] I. Yang and C. J. Tomlin, "Regularization-based identification for level set equations," *http://www.eecs.berkeley.edu/Pubs/TechRpts/2013/EECS-2013-156.pdf*, 2013.

[26] L. C. Evans, *Partial Differential Equations*, 2nd ed. American Mathematical Society, 2010.

[27] J. Nocedal and S. Wright, *Numerical Optimization*, 2nd ed. New York, NY: Springer, 2006.

[28] W. Hundsdorfer and J. G. Verwer, *Numerical Solutions of Time-Dependent Advection-Diffusion-Reaction Equations*. Springer, 2007.

[29] R. H. Byrd, M. E. Hribar, and J. Nocedal, "An interior point algorithm for large-scale nonlinear programming," *SIAM Journal on Optimization*, vol. 9, no. 4, pp. 877–900, 1999.

[30] R. A. Waltz, J. L. Morales, J. Nocedal, and D. Orban, "An interior point algorithm for nonlinear optimization that combines line search and trust region steps," *Mathematical Programming*, vol. 107, pp. 391–408, 2006.

[31] A. F. M. Marée, A. Jilkine, A. Dawes, V. A. Grieneisen, and L. Edelstein-Keshet, "Polarization and movement of keratocytes: a multiscale modelling approach," *Bulletin of Mathematical Biology*, vol. 68, pp. 1169–1211, 2006.

[32] E. L. Barnhart, K.-C. Lee, K. Keren, A. Mogilner, and J. A. Theriot, "An adhesion-dependent switch between mechanisms that determine motile cell shape," *PLoS Biology*, vol. 9, no. 5, pp. 1–19, 2011.